J Mater Sci: Mater Med (2008) 19:407–415
DOI 10.1007/s10856-007-3172-9

Bone-like matrix formation on magnesium and magnesium alloys

Alexis Pietak · Patricia Mahoney · George J. Dias · Mark P. Staiger

Received: 22 May 2006 / Accepted: 11 September 2006 / Published online: 3 July 2007

Abstract Mg metal and its alloys have promise as a biocompatible, degradable biomaterials. This work evaluates the potential of in vitro cell culture work with osteoblast-like cells on Mg based materials, and investigates cell differentiation and growth on Mg alloyed with various non-toxic or low-toxicity elements. Mg based substrates support the adhesion, differentiation and growth of stromal cells towards an osteoblast-like phenotype with the subsequent production of a bone like matrix under in vitro conditions. No significant difference in the final tissue layer is observed on pure Mg, an AZ21 alloy or a 0.5 wt% Ca alloy. Only a 0.8 wt% Ca alloy which shows complete structural disintegration shows minimal cell growth. Due to association of non-soluble degradation products formed when Mg is incubated in physiological-like fluid, mass changes typically used to report Mg degradation are not viable estimates of degradation. Methods quantifying the time dependent change in the mechanical integrity of samples as a function of incubation time are required for a proper assessment of Mg degradation. We conclude that in vitro cell culture of bone cells on Mg substrates is expected to be a viable screening technique to assess the relative biological activity of Mg-based materials.

A. Pietak (✉) · M. P. Staiger
Department of Mechanical Engineering,
University of Canterbury, Private Bag 4800,
Christchurch, New Zealand
e-mail: alexis.pietak@gmail.com

P. Mahoney · G. J. Dias
Department of Anatomy & Structural Biology,
University of Otago Medical School,
P.O. Box 913, Dunedin, New Zealand

Introduction

Metals offer unrivaled mechanical properties for the repair of load bearing defects in skeletal tissue. Materials such as titanium and surgical steel are commonly used in orthopeadic applications. Possible drawbacks with the use of these materials are the introduction of toxic elements to the biological system [1–3], stress shielding resulting from a mismatch between the mechanical properties of the metal and osseous tissue [4], and that the implants remain as permanent fixtures, requiring removal with secondary surgery after the tissue has healed.

Magnesium (Mg) metal and its alloys offer intriguing solutions to existing issues with conventional metal implant materials [5]. At a density of 1.74 g/cm^3, Mg is among the most lightweight of metals [6] with mechanical properties similar to natural bone [5]. Mg readily degrades in vivo [7], however as Mg ions are the fourth most prevalent constituent of human serum [8] the degradation products are expected to be non-toxic. Mg ions have a natural presence in osseous tissue and deficiency studies have indicated elemental Mg is required for healthy skeletal development and maintenance [9–13]. Thus, Mg metal based materials have the potential to serve as biodegradable metal scaffolds suitable for repair of load-bearing defects in osseous tissue, with less chance of stress shielding effects observed with use of higher modulus materials such as titanium [5]. In addition Mg implants may demonstrate higher biological activity than conventional metals as has been indicated by various studies involving Mg-doped biomaterials [13–16].

The main limitation in the implementation of Mg as an orthopeadic biomaterial is that degradation occurs before the formation of stable tissue around the implant [5]. Alloying Mg is necessary to improve corrosion resistance

[17]. However, for the application of a degradable implant, alloying elements must be chosen with careful consideration of the possible systemic effects resulting from their introduction to the physiological system. Negative effects of elements leached from much more stable implants such as Ti alloys are observed [2, 3, 18, 19]. Elements commonly chosen to improve corrosion resistance of Mg are Ni, Al, Zr, Y and Nd [17, 20, 21]. A wealth of data points to severe adverse systemic effects of Al [18, 22–24]. Ni and Zr have known chronic toxicity [25]. The systemic effects of Y, Nd and other rare-earth elements have not been extensively studied[1].

Although it is claimed that Mg is a potential biomaterial for orthopeadic applications, only a sparse body of research evaluating cell and tissue growth on Mg and its alloys is in existence [5]. Very significantly, a number of in vivo studies have confirmed that Mg and its alloys show promise as slow-degrading orthopaedic implants [7, 26–29]. While it is true that in vivo testing is the state of the art for evaluation of a biomaterial, it is a slow, expensive and intensive procedure. In vitro testing allows for a more exhaustive exploration of cell growth and activity on Mg and its alloys at this early stage of research into biological interactions. As far as the authors are aware there are no published results of bone cell growth and performance on Mg metal and its alloys under in vitro conditions.

The present findings from in vitro cell culture work on various Mg based substrates demonstrate that Mg and Mg alloy surfaces support the adhesion, differentiation, and proliferation of stromal cells to an osteoblast-like phenotype with production of a bone-like matrix. The work also evaluates the effect of various non-toxic or low-toxicity alloying elements on Mg degradation and cellular response under in vitro conditions.

Experimental

Materials

Commercially pure Mg ingots (99.8% - Glucina Smelters, Auckland) were used as sample group A1, and in preparation of Ca–Mg alloys. Mg alloys with desired compositions of 0.5 wt% and 1.5 wt% Ca were prepared by heating Mg and Ca metal in a vacuum furnace at 700 °C. Chemical analysis for Ca in the resulting alloys (Spectometer Services Pty. Ltd.) indicated that the actual composition of the alloys were 0.51 wt% (sample group A3) and 0.81 wt% Ca (sample group A4).

In addition to the above samples a commercially prepared Al-Zn Mg alloy (Glucina Smelters, Auckland) containing 2% Al and 1% Zn was included in the study (sample group A2) to compare the performance of a material alloyed with elements known to enhance corrosion resistance of Mg [21].

Preparation of the Mg metal involved cutting disks 1 cm in diameter and 3 mm in thickness from Mg or Mg alloy ingots. The surfaces of the disks were abraded with Si-C 800 grit paper to generate a surface with some roughness for enhanced cell adhesion.

Table 1 provides a summary of sample indexing and corresponding descriptions.

Degradation testing

Degradation of Mg based materials in tissue culture media was assessed on the basis of mass changes after 8 days incubation in 24 well cell culture plates in 1 mL of cell culture media at 37 °C and 5% CO_2. The composition of the cell culture media was identical to that used in cell culture and is described in section 2.3. Fluid was changed in the degradation samples at the same intervals as for the samples cultured with cells, once every 2–3 days.

Rat stromal cell culture

Osteoblast-like cells were derived from dexamethasone induced differentiation of stromal cells obtained from bone marrow washes of young male rats [30, 31]. Four male Wistar rats weighing 100–110 g were euthanized using CO_2. Femurs were surgically removed under aseptic conditions and immediately transferred to an ice-cold cell culture medium containing α-MEM (GIBCO) supplemented with 15% fetal calf serum (growth factors) (FCS, Sigma), antibiotics 1 mg/mL Penicillin (Sigma), 50 μg/mL Gentamycin (Sigma), and anti fungal agent 3 μg/mL Nystatin (Sigma). Under sterile conditions the epipheses of the femur were cut and the medullary canal was exposed by puncturing with a 20 g hypodermic needle. Bone marrow was extracted by flushing each medullary canal with 10 mL of cell culture media composed of α-MEM (GIBCO) supplemented with 15% fetal calf serum (FCS, GIBCO), 0.1 mg/mL Penicillin (Sigma), 50 μg/mL Gentamycin (GIBCO), 0.3 μg/mL Nystatin (GIBCO), 70 μg/mL ascorbic-acid-2-phosphate, 2 mg/mL β-glycerol phosphate (Sigma) and 4 ng/mL Dexamethasone (Sigma), using a hypodermic needle. After dispersion of cell clumps and passing the suspension through a cell-sieve, 5 mL of the resulting suspension of cells were seeded onto tissue culture treated flasks (Corning co-star) and sub-cultured to confluence after 5 days of growth in a tissue culture incubator at 5% CO_2 and 37 °C. Cells were extracted from the flasks using a solution of trypsin-EDTA, centrifuged at 1100 rpm for 10 min and re-suspended in cell culture media. After

[1] http://en.wikipedia.org/wiki/Neodymium

Table 1 Experimental matrix

Sample index	Sample description	Degradation in situ	ALP activity	Total protein	Images of cultured surface
A1	99.9% Pure Mg	Low reactivity. Small mass increase (<1%)	Mean decrease; statistically equivalent to control	Equivalent to control	Granular top matrix composed of ~20 nm crystals, inner mesh of ~30 nm diameter smooth fibers with ~90 nm globules. Cell like structures visible in confocal microscopy
A2	AZ21 alloy	Low reactivity. Small mass increase, small pH change	Mean decrease; statistically equivalent to control	Equivalent to control	Same as A1, however regions of globular structure with OCP-like crystal precipitation on top layer.
A3	0.5 wt% Ca alloy	Reactive. 11% Mass increase	Significantly below control	Significant decrease	Similar to A1
A4	0.8 wt% Ca alloy	Physical disintegration, small mass loss	Significantly below control	Mean decrease; statistically equivalent to control	Not examined
S	Tissue culture treated control slide	/	/	/	Top-layer of polygonal cells 15–20 μm in diameter

cell counting using a hemocytometer, cells were diluted to a seeding concentration of 1×10^4 cells/mL. One mL of cell suspension was seeded to ethanol disinfected Mg-based disks in tissue culture treated wells of a 24 well plate (Corning Costar). The positive control group consisted of 1 cm diameter tissue-culture treated slides (Thermonox, Nunc Brand), referred to as sample group 'S'. All samples were incubated with 5% CO_2 at 37 °C. Medium in the culture was changed every 2–3 days.

Alkaline phosphatase and total protein assay

After 8 days of culture four sample replicates per group were washed thoroughly with PBS, and cells were lysed by freezing and thawing in a buffer solution containing 0.1 M glycine, 0.01 M $MgCl_26H_2O$, and 0.1% Triton-X. The resulting suspension was centrifuged to remove cellular debris. Total protein in the solution was measured using the Quantipro BCA assay kit (Sigma).

Alkaline phosphatase activity was measured using the p-nitrophenol assay in which para-nitrophenyl phosphate (pNpp), a colorless substrate, is hydrolyzed by alkaline phosphatase at pH 10.5 and 37 °C to yellow para-nitrophenol (pNp) (using the world health organization protocol [32] based on the work of Bowers and McComb [33]). A calibration curve for alkaline phosphatase activity concentration in units of μM of enzyme activity per minute per liter (U/L) was prepared by diluting a 50 μM standard solution of pNp (Sigma) in 0.20 M NaOH. A total of 10 μl of sample was mixed with 200 μl of pNpp substrate in 2-amino-2-methyl-1-propanol buffer at pH 10.5 (Sigma) in a 95 well plate, and incubated at 37 °C for 15 min. The reaction was stopped with the addition of 40 μl of 0.25 M NaOH. The plate was read on a microplate reader (Bio-Rad) at a light wave length of 415 nm.

A one tailed student-t test at a $p < 0.05$ level of significance has been used to determine if a difference exists between the mean of two populations of data that have undergone different experimental treatments.

Field-Emission Scanning Electron Microscopy (FE-SEM)

After 17 days of cell culture samples for FE-SEM microscopic investigation were washed thoroughly in PBS and were fixed in 2% glutaraldehyde in 0.1 M Na-Cacodylate buffer. Samples were dehydrated using an alcohol series and freeze-dried. A total of 10 nm of gold was sputtered onto the samples using an Emitech K3575 high-resolution sputter coater. FE-SEM was performed on a JEOL JSM-6700F. The surface chemistry was investigated using energy-dispersive-X-ray spectroscopy (EDS) on carbon-coated samples on a JEOL JSM-7000F FE-SEM with beam energy of 10 keV.

Confocal microscopy

After 17 days of cell culture, samples for confocal microscopic investigation were washed thoroughly in PBS and fixed in 5% glutaraldehyde for 12 h at 4 °C. Confocal microscopy was performed on a Zeiss LSM 510 confocal laser scanning microscope. An air cooled argon laser operating at 1.5 mW was used to induce auto-fluorescence in glutaraldehyde fixed samples at a wavelength of 488 nm.

Samples were viewed using a 63× objective with a 6.4 μs pixel time and a 2.9 μm pinhole.

Results

Degradation in culture medium

Optical images of metal surfaces after 8 days incubation in tissue culture media at 37 °C and 5% CO_2 are shown in Fig. 1. The original metal has a highly reflective scratched surface, Fig. 1A. After incubation sample A4 undergoes catastrophic structural failure, and a white precipitate can be clearly seen coating the remaining fragments, Fig. 1D. The surfaces of samples A1 and A2 appear relatively unreactive in media loosing the original luster, however scratch marks are still visible from the initial preparation, Fig. 1B. The surface of A3 shows a significant amount of white precipitate on the surface, Fig. 1C.

Changes to the mass of the samples after incubation, Fig. 2, reflect the changes observed with optical inspection. It is clear that Mg based materials are fairly reactive in the electrolytic cell culture media and do not simply transform into $MgCl_2$ and wash away, loosing mass in the process. From Fig. 1 it is apparent that degradation/precipitation products remain associated with the samples. It is not possible to determine the degree of sample degradation on the basis of mass changes. In all cases except for the complete disintegration of sample A4, mass increases corresponding to the degree of degradation/precipitation formation are observed, Fig. 2.

Biological activity

The tissue culture plate at day 8 of cell growth, prior to the media change, Fig. 3, qualitatively shows variations in pH through phenol red included in culture media, which ranges from yellow-purple over the pH range 6–8. The control slide ('S' sample group) shows slightly acidic conditions typical of the metabolic activity of healthy cell growth in the well. In comparison to the control group, sample groups A1–A3 are increasingly more basic, which may be associated with hydroxide products from Mg sample corrosion in the media. The media in the group of A4 is remarkably basic and is obviously associated with a severe and rapid corrosion of the sample. This is expected to have a strong inhibitory effect on cell growth. Due to the severe degradation of sample A4, no further microscopic investigations were conducted on these samples.

Confocal microscopy images of samples are shown in Fig. 4. A representative acellular control sample clearly shows the original scratch marks of sample preparation and some small patches of corrosion product, Fig. 4A. In the case of samples cultured with cells, it was possible to visualize slices of the tissue layer passing from the top of the layer down to the metal surface where scratch marks from the original sample preparation were a visible, indication of reaching the end of the tissue layer. All samples showed a top layer comprised of polygonal cells 15–20 μm in diameter with numerous short filamentous structures extending from the boundary—characteristic features of osteoblast-like morphology [34]. These features are indicated by 'O' in the panels. This characteristic top layer is

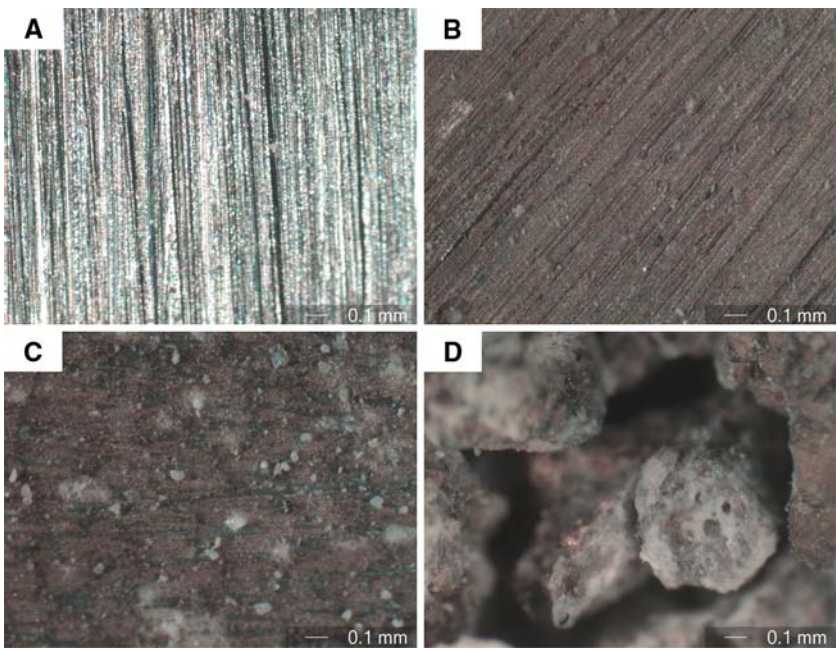

Fig. 1 Optical images of metal surfaces after 8 day incubation in tissue culture media at 37 °C and 5% CO_2. Panel **A** shows the original, highly reflective morphology of the metal surface. Panel **B**, **C** and **D** show the surfaces of samples A1, A3 and A4 after the 8 day incubation

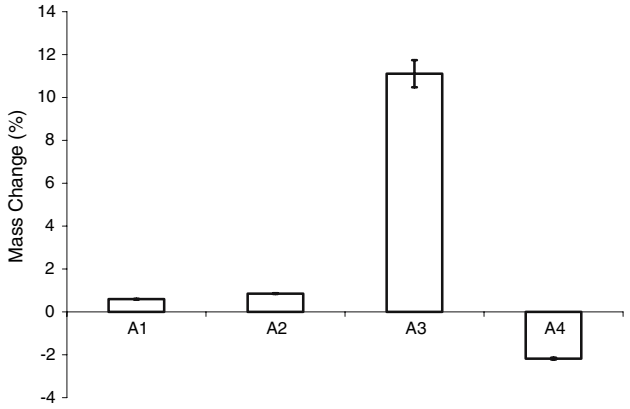

Fig. 2 Mass changes after 8 days incubation in cell culture media at 37 °C and 5% CO2

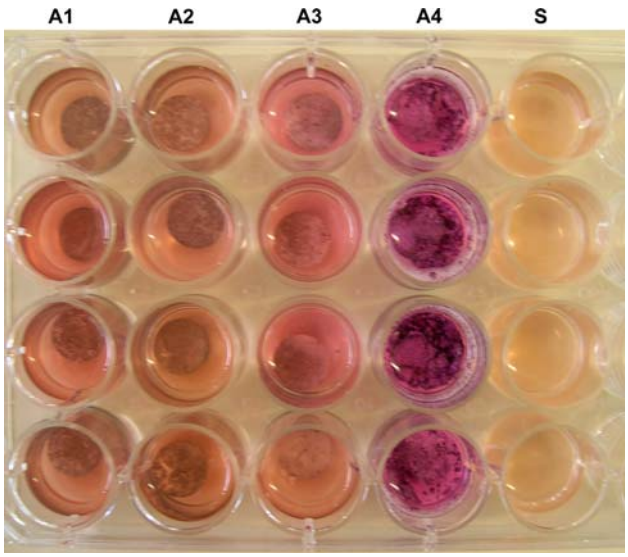

Fig. 3 Tissue culture plate at day 8 prior to media change showing variations in pH with samples associated with corrosion in media. Samples are grouped as columns in groups of 4

shown in Fig. 4B and E, for samples A3 and A1, respectively. Sample A3 shows a unique middle layer (Fig. 4C) composed of more elliptical cells, indicated by 'E', joined by fibrous structures, indicated by white arrows. Figure 4D and 4F show the characteristic morphology of the scratched metal surface for the A3 and A1 samples, respectively. On the basis of the number of steps taken to reach the metal substrate from the top surface of the sample, the tissue thickness on the substrates is between 30–40 μm. Control slides (group S, not shown) display nearly identical tissue morphology to sample A1.

FE-SEM images of sample surfaces are shown in Fig. 5. A typical acellular control surface for samples A1, A2 or A3 after 18 days of incubation is shown in Fig. 5A revealing a cracked corrosion-effected surface. Figure 5B shows hexagonal needle-like corrosion product also forming on acellular control surfaces. EDS analysis of this product, Table 2, shows it is rich in Mg and O. Figure 5C shows the typical morphology of tissue formed on samples A1–A3, showing a top layer consisting of osteoblast-like cells [34], indicated by 'T' and between the gaps of these cells a highly fibrous middle section is revealed, indicated by 'F'. Figure 5D shows close-up of the fibrous layer. EDS analysis of these fibers show they are primarily C, with traces of P and Ca that indicate possible mineralization of the surface. There were no remarkable differences in the tissue layer formed on the different alloys used in this study. Under FE-SEM, control slides (group S, not shown) display the same tissue morphology of a top layer of polygonal cells upon a fibrous substructure.

FE-SEM images of the A2 sample surface show in addition to the cellular top layer 'T' and the mineralized fibrous mid-layer 'F', expanses of globular clusters of crystals 'G', Fig. 6A. These are shown in close-up in panel B. The plate-like crystals arranged in a rosette cluster are typical of biomimetically precipitated hydroxyapatite (HA) or octacalcium phosphate (OCP) [35, 36] and were observed in some regions on all samples. EDS analysis of these globular clusters, Table 2, shows they are rich in Ca and P, supporting the identification as HA or OCP.

Our cell culture technique uses dexamethasone to induce the differentiation of stromal cells to an osteoblast phenotype [30]. It is assumed that the control slides (group S) provide ideal conditions for osteoblast-like cell growth and that the alkaline phosphatase (ALP) activity of these samples is a benchmark for differentiation of stromal cells to the osteoblast-like phenotype. Changes to the protein normalized ALP activity of Mg-based samples in comparison to the control group are therefore representative of the osteogenic capacity of the Mg substrates. ALP activity, normalized to total protein at day 8 of cell culture with 4 replicates per group is shown in Fig. 7. Average activity for all Mg-based sample groups is lower than that of the control substrate, however only groups A3 and A4 show statistically significant decreases, with $0.005 > p > 0.001$ for A3 samples and $0.001 > p$ for A4. The total protein at day 8 of cell culture is also lower on samples A3 and A4 in comparison to the control, indicating a decrease in cellular growth and metabolic activity on these groups, while samples A1 and A2 remain similar to the control group. Fig. 8.

A summary of the cell growth characteristics for the sample set is given in the experimental matrix of Table 1.

Discussion

On the basis of visual inspection and mass increases to materials, degradation/precipitation products remain asso-

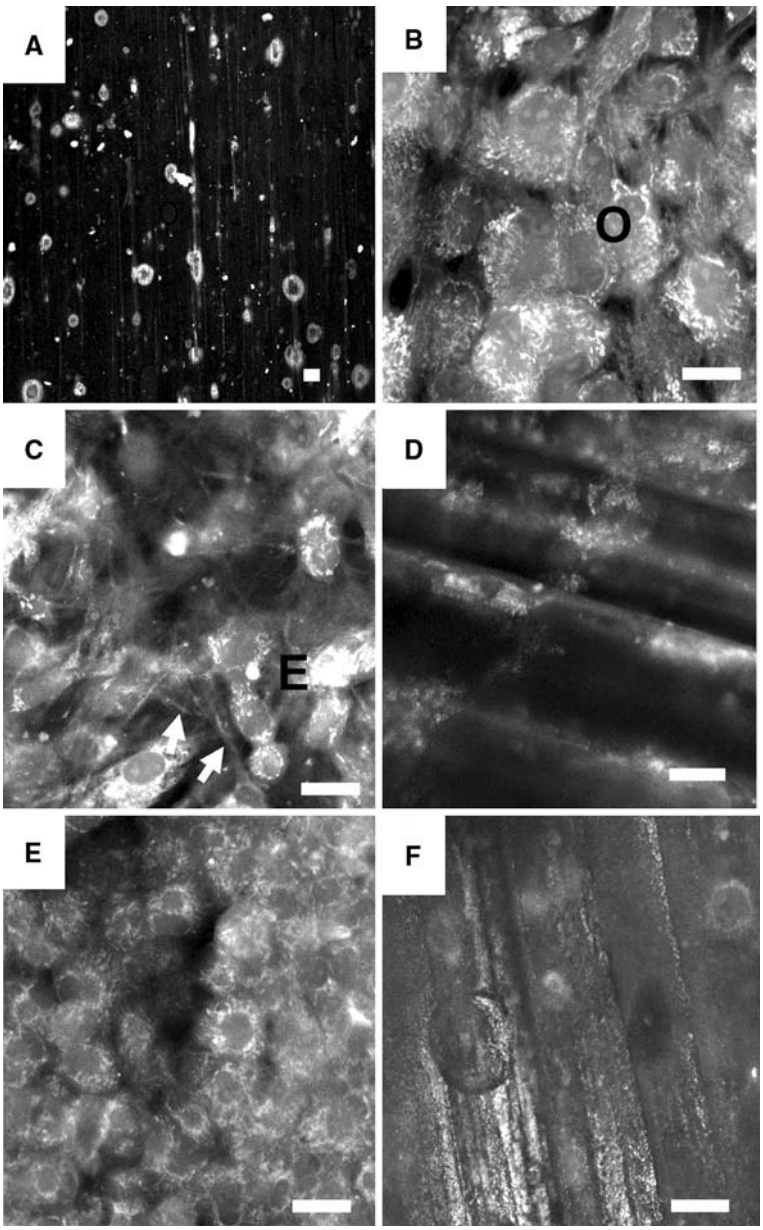

Fig. 4 Confocal microscopy images of samples. Panel **A** shows a representative acellular control sample. Panel **B**, **C** and **D** show the top, middle and bottom layer of the A3 sample. Osteoblast-like cells are marked with 'O', the elliptical cells with 'E' and fibrous structures indicated by white arrowheads. Panel **E** and **F** show the top and bottom surface of the Mg metal disk, A1. Scale bar shows 20 μm

ciated with the Mg samples leading to a mass increase of the samples. Estimates of Mg degradation based on mass changes are therefore not reliable for samples in more complex electrolytes similar to physiological fluids.

Witte et al. [37] have shown that assessment of the degradation of Mg results in significantly contradictory values for different alloys using different methods (mass changes, electrochemical) and in different environments (in vitro, in vivo). Degradation in vivo is expected to be significantly different to the in vitro case due to a strongly altered diffusion situation in vivo, where liquids are enclosed in cell membranes as well as around tissues and elements are removed by scavenger cells and the blood and lymphatic circulatory systems. A comprehensible measurement of in vitro corrosion, that is one that is uninfluenced by associated degradation/precipitation products, should still provide useful information for the study of the relative integrity of a series of Mg based materials. We propose the best measure of the relevant degradation of Mg based materials is through measurement of the mechanical integrity of samples as a function of incubation time in SBF [38]. In addition, time dependent pH measurements and measurements of Mg^{2+} concentration in media would help give a more clear indication of the effect of degradation on cellular activities for a corresponding group.

It is clear from microscopic investigations that Mg based substrates support the differentiation and proliferation of

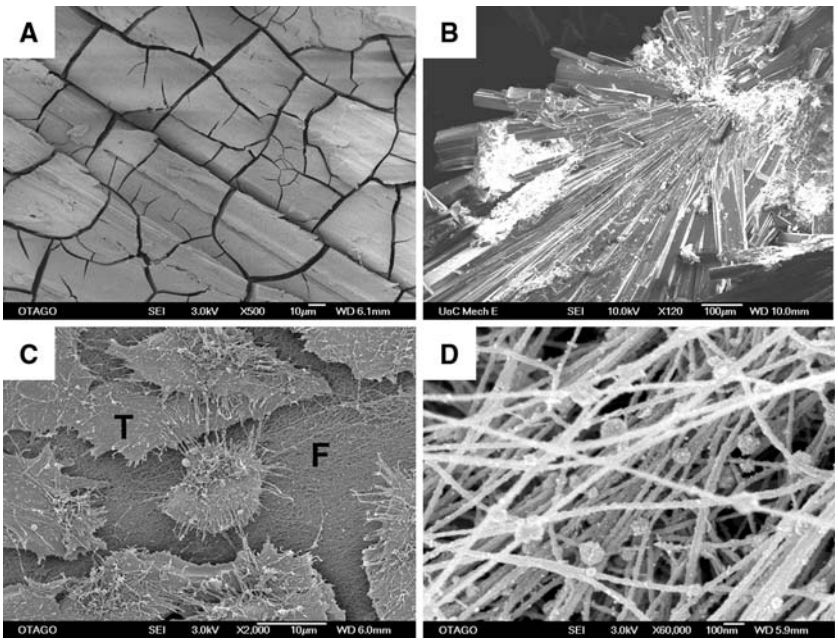

Fig. 5 FE-SEM images of sample surfaces. A typical acellular control surface for samples A1, A2 or A3 after 18 days of incubation is shown in panel **A**. Panel **B** shows crystalline degradation products. Panel **C** shows the morphology of tissue formed on samples A1, A2 and A3, showing a top layer of osteoblast-like cells indicated by T, and fibrous midsection, indicated by F. Panel **D** is a close-up of the fibrous structures

Table 2 Chemical composition of biotested samples determined using EDS

Sample	Mg (At%)	Ca (At%)	P (At%)	O (At%)	C (At%)	Na (At%)
Fiber (Fig 5D)	4.1	0.1	5.9	20.7	63.3	1.7
Degradation (Fig 5B)	10.1	0.0	0.0	66.6	23.3	0.0
Globule (Fig 6)	1.5	13.6	8.8	51.9	23.7	0.4

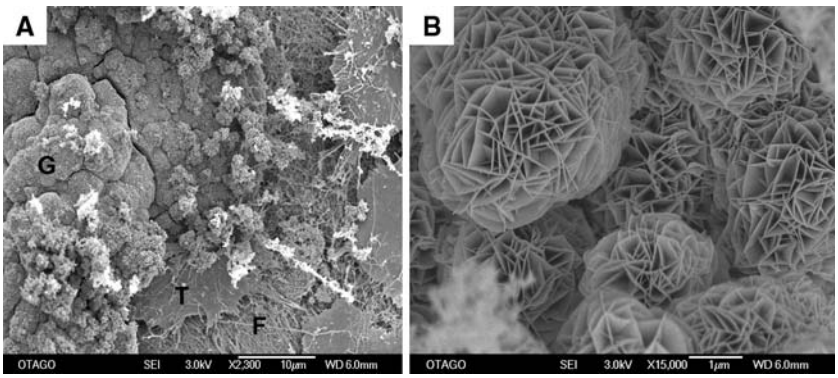

Fig. 6 FE-SEM images of the A2 sample surface which show in addition to the dense top layer T and the fibrous mid-layer F, globular clusters of a precipitate G, which is shown in close-up in panel **B**

stromal cells to an osteoblast-like phenotype, with the associated production of a mineralized matrix on the samples, however activity is somewhat compromised in comparison to the control group S. From confocal and FE-SEM images, the matrix visible in sample groups A1–A3 has a morphology typical of mineralized bone-like matrix that forms in vitro using dexamethasone induced rat stromal cells [30, 31, 39, 40]. However, the inner fibrous mesh has a morphology of a pre-collagen as fibers are thinner (~40 nm diameter) and have no signs of the banding typical of collagen I [41, 42]. The detection of low levels of P and Ca on the fibers suggests possible mineralization (Table 2). On the basis of ALP measurements, the Mg based substrates demonstrate significant ALP activity, however they are less osteogenic in comparison to the control slides. The degree of these changes is associated with the reactivity of Mg substrates in culture media, where sustained increases in pH and ion concentration presumably affect the cell differentiation, proliferation, and function. Such extensive changes in pH and ion concentrations would not be expected in vivo due to degradation products being efficiently evacuated from the implantation site by scavenger cells and blood and lymphatic circulatory systems and the buffering action of the tissue fluid.

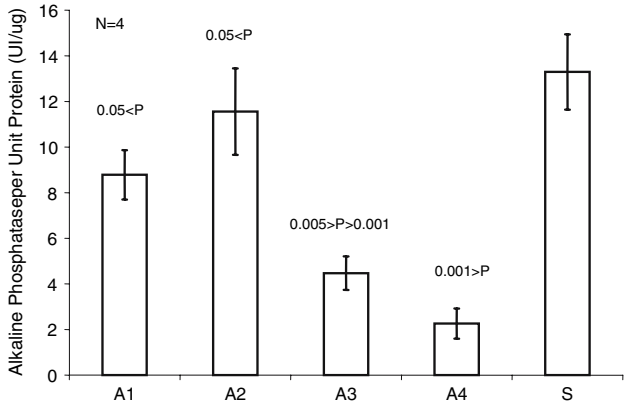

Fig. 7 Alkaline phosphatase activity, normalized to total protein at day 8 of cell culture with 4 replicates per group. A student-*t* test was used to compare the mean ALP activity of each sample to the control slide substrate S, with respective P values shown on the graph

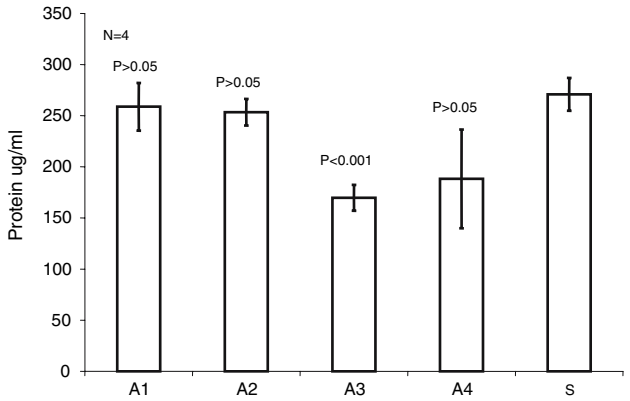

Fig. 8 Total protein at day 8 of cell culture with 4 replicates per group. A student-*t* test was used to compare the mean of each sample to the control slide substrate S, with respective P values shown on the graph

Research by Witte et al. [37] has determined that Mg is expected to be up to three orders of magnitude more reactive under in vitro conditions rather than in the in vivo environment. As the in vitro conditions therefore represent a more harsh case for cell growth and function in comparison to the behavior of Mg in vivo, exaggerated relative differences in the biological performance of cells cultured in vitro on Mg substrates are to be expected.

Conclusions

This study concludes that in vitro culture of bone cells on Mg based substrates is a feasible endeavor. Mg based substrates support the adhesion and differentiation of stromal cells towards an osteoblast-like phenotype with the subsequent production of a bone like matrix under in vitro conditions. Alloys AZ21 and pure Mg show the best results in terms of alkaline phosphatase activity. No discernable morphological differences were observed in the final tissue layer of samples A1–A3. The 0.8 wt% Ca alloy, group A4 disintegrates rapidly with incubation in cell culture media and is therefore not a viable option for a low-toxicity Mg alloy biomaterial. Mass changes typically used to report Mg degradation are not viable estimates of degradation in the electrolytic environment of physiological-like fluids due to association of non-soluble degradation products. Methods quantifying the time dependent change in the mechanical integrity of samples as a function of incubation time in SBF [38] and the pH and Mg^{+} ion changes to the culture are required for a proper assessment of Mg degradation and sample reactivity in media. The formation of bone-like matrix on samples A1–A3 is a highly encouraging result, suggesting in vitro culture conditions can be used to screen the biological performance of Mg metal-based materials for orthopaedic applications.

Acknowledgments This work was financially supported by the Brian Mason Scientific & Technical Trust and University of Canterbury Grants U6513 and U6568. Thank you to Dr. David Aitchison for support. The authors also thank Mr. K. Stobbs, Mr. M. Flaws (Mechanical Engineering University of Canterbury) for technical assistance.

References

1. M. ALLEN, B. MYER, P. MILLET and N. RUSHTON, *J. Bone Joint Surg.* **79-B**, (1997) 475
2. Y. BI, R. VAN DE MOTTER, A. RAGAB, V. GOLDBERG, J. ANDERSON and E. GREENFIELD, *J. Biomed. Mater. Res.* **83** (2001) 501
3. J. JACOBS, J. HALLAB, A. SKIPOR and R. URBAN, *Clin. Ortho. Rel. Res.* **417** (2003) 139
4. J. NAGELS, M. STOKDIJK and P. ROZING, *J. Shoulder Elbow Surg.* **12** (2003) 35
5. M. STAIGER, A. PIETAK, J. HUADMAI and G. DIAS, *Biomaterials* **27** (2006) 1728
6. P. DEGARMO, in "Materials and Processes in Manufacturing" (Collin Macmillan Int. Ed., NY, 1979)
7. F. WITTE, B. MICHAEL, M. KLEMENT, F. GOEDE, C. WIRTH and H. WINDHAGEN, 51st Annual Meeting of the Orthopaedic Research Society, 2005
8. J. VORMANN, *Mol. Asp. Med.* **24** (2003) 27
9. J. VORMANN, C. FORSTER, U. ZIPPEL, E. LOZO, T. GUNTHER, H. MERKER and R. STAHLMANN, *Calcif. Tissue Int.* **61** (1997) 230
10. T. OKUMA, *Nutrition* **17** (2001) 679
11. R. RUDE, M. KIRCHEN, H. GRUBER, M. MEYER, J. LUCK and D. CRAWFORD, *Magnes. Res.* **12** (1999) 257
12. G. STENDIG-LINDBERG, R. TEPPER and I. LEICHTER, *Magnes. Res.* **6** (1993) 155
13. C. HOWLETT, H. ZREIOAT, R. O'DELL, J. NOORMAN, P. EVANS, B. DALTON, C. MCFARLAND and J. STEELE, *J. Mater. Sci: Mater. Med.* **5** (1994) 715
14. C.M. SERRE, M. PAPILLARD, P. CHAVASSIEUX, J. C. VOEGEL and G. BOIVIN, *J. Biomed. Mater. Res.* **42** (1998) 626

15. H. ZREIQAT, C. HOWLETT, A. ZANNETTINO, P. EVANS, G. SCHULZE-TANZIL, C. KNABE and M. SHAKIBAEI, *J. Biomed. Mater. Res.* **62** (2002) 175
16. Y. YAMASAKI, Y. YOSHIDA, M. OKAZAKI, A. SHIMAZU, T. UCHIDA, T. KUBO, Y. AKAGAWA, Y. HAMADA, J. TAKAHASHI and N. MATSURA, *J. Biomed. Mater. Res.* **62** (2002) 99
17. B. SHAW, Corrosion resistance of magnesium alloys. "ASM Handbook Voume 13 A:Corrosion:Fundamentals, Testing and Protection". D. STEPHEN (ASM Int., United Kingdom, 2003)
18. G. THOMPSON and D. PULEO, *Biomaterials* **17** (1996) 1949
19. M. WANG, L. NESTI, R. TULI, J. LAZATIN, K. DANIELSON, P. SHARKEY and R. TUAN, *J. Ortho. Res.* **20** (2002) 1175
20. V. KAESEL, P.T. TAI, Fr.-W. BACH, H. HAFERKAMP, F. WITTE and H. WINDHAGEN 6th International Conference Magnesium Alloys and Their Applications, (Wiley-Vch, 2006)
21. G. SONG and A. ATRENS, *Adv. Eng. Mater.* **5** (2003) 837
22. J. JOSHI, *Biofactors* **2** (1990) 163
23. O. ANDERSON and J. DAHL, *Biomaterials* **15** (1994) 882
24. C. HEWITT, J. SAVORY and M. WILLS, *Clin. Lab. Med.* **10** (1990) 403
25. V. CHASHSCHIN, P. ARTUNINA and T. NORSETH, *Sci. Total Env.* **148** (1994) 287
26. F. WITTE, V. KAESE, H. HAFERKAMP, E. SWITZER, A. MEYER-LINDENBERG, C. WIRTH and H. WINDHAGEN, *Biomaterials* **26** (2005) 3557
27. F. WITTE, F. GOEDE, J. FISCHER, H.A. CROSTACK, J. NELLESEN, F. BECKMANN, C.J. WIRTH, M. RUDERT and H. WINDHAGEN, 51st Annual Meeting of the Orthopaedic Research Society (2005)
28. A. LAMBOTTE, *Bulletin et Mém de la Soc Nat de Chir* **28** (1932) 1325
29. E. MCBRIDE, *D. J. Am. Med. Ass.* **111** (1938) 2464
30. C. MANIATOPOULOS, J. SODEK and A. MELCHER, *Cell. Tissue Res.* **254** (1988) 317
31. S. LANGSTAFF, M. SAYER, T. SMITH and S. PUGH, *Biomaterials* **22** (2001) 135
32. WORLD HEALTH ORGANIZATION, in "Standard operating procedures for clinical chemistry - alkaline phosphatase" (http://www.w3.whosea.org/EN/Section10/Section17/Section53/Section481_1761.htm, 2006)
33. G. BOWERS and R. MCCOMB, *Clin. Chem.* **21** (1975) 1988
34. R. KRSTIC, in "General Histology of the Mammal" (New York, Springer-Verlag, 1984) p. 133
35. U. SAMPATHKUMARAN, M. DEGUIRE and R. WANG, *Adv. Eng. Mat.* **3** (2001) 401
36. F. BARRER, P. LAYROLLE, C.A. Van BLITTERWWIJK and K. De GROOT, *Bone* **25** (1999) 107S
37. F. WITTE, J. FISCHER, J. NELLESEN, H. CROSTACK, A.V. KAESE, A. PISCH, F. BECKMANN and H. WINDHAGEN, *Biomaterials* **27** (2006) 1013
38. G. DIAS and P. PEPLOW, *J. Mater. Sci: Mater. Med.* **15** (2004) 1217
39. M. MULARI, R. QU, P. HARKONEN and H. VAANANEN, *Calcif. Tissue Int.* **75** (2004) 253
40. A. BOYDE and M. HOBDELL, *Z. Zellforsch* **93** (1969) 213
41. G. OWEN, M. KAAB and K. ITO, *Scanning Microscopy* **13** (1999) 83
42. D. KEEN, L. SAKAI and R. BURGESON, *J. Histochem. Cytochem.* **39** (1991) 59